Proceedings of the Seventh International ASME Conference on Nanochannels, Microchannels and Minichannels
ICNMM2009
June 22-24, 2009, Pohang, South Korea

ICNMM2009-82080

INVESTIGATING THE EFFECT OF SOLID BOUNDARIES ON THE GAS MOLECULAR MEAN-FREE-PATH

Erik J. Arlemark* **and Jason M. Reese**
Department of Mechanical Engineering
University of Strathclyde
Glasgow, G1 1XJ
United Kingdom
Email: erik.arlemark@strath.ac.uk / jason.reese@strath.ac.uk

ABSTRACT

A key parameter for micro-gas-flows, the mean free path, is investigated in this paper. The mean free path is used in various models for predicting micro gas flows, both in the governing equations and their boundary conditions. The conventional definition of the mean free path is based on the assumption that only binary collisions occur and is commonly described using the macroscopic quantities density, viscosity and temperature. In this paper we compare the prediction by this definition of the mean free paths for helium, neon and argon gases under standard temperature and pressure conditions, with the mean free paths achieved by measurements of individual molecules using the numerical simulation technique of molecular dynamics. Our simulation using molecular dynamics consists of a cube with six periodic boundary conditions, allowing us to simulate an unconfined gas "package". Although, the size of this package is important, since its impact on computational cost is considerable, it is also important to have enough simulated molecules to average data from. We find that the molecular dynamics method using 20520 simulated molecules yields results that are within 1% accuracy from the conventional definition of the mean free paths for neon and argon and within 2.5% for helium. We can also conclude that the normal approximation of only considering binary collisions is seemingly adequate for these gases under standard temperature and pressure conditions. We introduce a single planar wall and two parallel planar walls to the simulated gas of neon and record the mean free paths at various distances to the walls. It is found that the mean free paths affected by molecular collisions with the walls corresponds well with theoretical models up to Knudsen numbers of 0.2.

1 INTRODUCTION

As our interest in micro gas flow applications is growing with improved manufacturing capabilities it is also apparent that the conventional isothermal flow model consisting of the Navier-Stokes equations with no-velocity-slip boundary condition fail for such cases. This is because micro-gas-flows differ from macro-gas-flows with respect to the relatively large ratio of the confining boundary surface area to the volume of the confined gas, which means that certain additional surface effects must be taken into account. These surface effects considerably influence the flow in the near-wall region, the Knudsen-layer, which is about two mean free paths wide. A commonly used mean free path expression for molecules, is expressed in terms of the gas dynamic viscosity, μ, density, ρ, the specific gas constant R and temperature, T, as follows [1]:

$$\lambda = \frac{\mu}{\rho}\sqrt{\frac{\pi}{2RT}}, \tag{1}$$

given the assumption that the molecules have a Maxwellian velocity distribution. An other assumption of Eq. 1 is that the gas

*Address all correspondence to this author.

is sufficiently dilute i.e. molecules only experience binary collisions. A requirement for a gas to be dilute is:

$$\frac{d}{\delta} \ll 1, \tag{2}$$

where d is the molecular diameter and δ is the average distance between molecules [2].

The key parameter indicating the degree of departure from equilibrium, the Knudsen number (Kn), is then defined as:

$$Kn = \frac{\lambda}{l}, \tag{3}$$

where l is a measure of the geometrical-length-scale. In this paper the length scale l is the channel width between two planar walls.

Modelling the Knudsen-layer should ideally be performed using detailed kinetic theory. However an appropriate extension to the Navier-Stokes equations would be less time-consuming and less demanding of computational capacity. Flows up to $Kn \approx 0.1$ can be modelled by applying a velocity-slip to the conventional Navier-Stokes equations. Above $Kn \approx 0.1$ the assumption of a linear stress/strain-rate relationship breaks down as the Knudsen-layer covers an ever larger part of the flow-domain.

An investigation by Arlemark *et al.* [3] shows how a non-linear stress/strain-rate relationship can extend the applicability of the Navier-Stokes equations beyond $Kn \approx 0.1$. The non-linear relationship is obtained through using a theoretically and physically derived mean-free-path, which is geometry-dependent due to that it accounts for intermolecular gas collisions as well as gas collisions with solid boundaries.

The main purpose of this paper is therefore to assess the mean free path profile affected by solid walls by using molecular dynamics, and compare these results to the theoretical and physically derived definition of the mean free path in [3].

2 COMPARING MEAN FREE PATH OF NUMERICAL EXPERIMENT WITH THE CONVENTIONAL EXPRESSION

To begin with we compare the theoretical and constant mean free path value given by Eq. (1) for helium, neon and argon gas[1] at standard temperature and pressure (STP), with the corresponding mean free path values simulated by molecular dynamics. In table 1 we have listed the gas parameters used in Eq. (1) together with the acquired mean free path values.[2]

[1]We have chosen to model noble gases due to that they are monoatomic molecules, which makes them easier to interpret theoretically and to model using molecular dynamics

[2]The specific gas constant has been calculated using $R = R_u/M$, where R_u is the universal gas constant having the value of 8.3145 $[J/(kg \times K)]$.

Table 1. GAS DATA FOR STANDARD TEMPERATURE PRESSURE. [4]

Gas:	He	Ne	Ar
$\mu \times 10^6\,[J/(kg \times K)]$	18.2	29.7	20.8
$\rho\,[kg/m^3]$	0.178	0.900	1.784
$R\,[J/(kg \times K)]$	2077.3	412.2	208.1
$\lambda \times 10^7\,[m]$	1.696	1.233	0.613

To model the mean free paths of the noble gases we use the open source software OpenFOAM (Open Field Operation and Manipulation) [5] with the molecular dynamics routines implemented by G. Macpherson *et al.* [6, 7]. Although molecular dynamics is often used to model liquids at the nano scale we have here chosen to use this technique to model gases at STP.

2.1 The definition of collisions depends on intermolecular potential

In the molecular dynamics simulation we have chosen to use the Lennard-Jones interaction potential, Φ, given by:

$$\Phi = 4\varepsilon \left[\left(\frac{\sigma}{r_{ij}} \right)^{12} - \left(\frac{\sigma}{r_{ij}} \right)^{6} \right], \tag{4}$$

which acts on molecules i and j separated by a distance r_{ij}, where ε is related to the interaction strength of the molecules and σ corresponds to the distance at which the potential between the two molecules is zero [8]. We have chosen to set σ equal to the hard sphere diameter of a monatomic gas, which is determined by its relationship to viscosity according to R. Bird *et al.* [9] and G. Bird [10] as follows:

$$\sigma = \sqrt{\frac{5}{16} \frac{M}{N_{Av}\mu} \sqrt{\frac{RT}{\pi}}}, \tag{5}$$

where N_{Av} is Avogadro's number, 6.0221415×10^{23} and M is the molar mass, which for helium, neon and argon has the values of 4.003, 20.180 and 39.95 $[kg/kmol]$ respectively. For helium, neon and argon at STP Eq. (5) yield σ-values of $2.2023 \times 10^{-10}\,[m]$, $2.5830 \times 10^{-10}\,[m]$ and $3.6616 \times 10^{-10}\,[m]$ respectively. By using Eq. (5) it is then possible to calculate the kinetic value of the mean free path given by:

$$\lambda_k = \frac{M/N_{Av}}{\pi\rho\sigma^2\sqrt{2}}, \tag{6}$$

Table 2. Lennard-Jones parameter data. Prime notation distinguish commonly used data, where data for helium is from [9] and data for neon and argon is from [10]. The prime notated parameters are used here for scaling our applied ε.

Gas:	He	Ne	Ar
$\sigma' \times 10^{10}\,[m]$	2.576	2.720	3.405
$\varepsilon' \times 10^{22}\,[J]$	1.4083	6.4891	17.2857
$\sigma \times 10^{10}\,[m]$	2.2023	2.5830	3.6616
$\varepsilon \times 10^{22}\,[J]$	1.9654	7.1957	14.9480

which yields the values $1.727 \times 10^{-7}[m]$, $1.255 \times 10^{-7}[m]$ and $0.624 \times 10^{-7}[m]$ for helium, neon and argon respectively. It should be noted that the mean free path values from this derivation are approximately 2% higher than the values attained from Eq. (1) according to [2].

The parameter ε is chosen so that the reduced sound damping factor presented by E. Guarini *et al.* [11]:

$$\Gamma^* = \frac{\Gamma}{\sigma}\sqrt{M/\varepsilon}, \tag{7}$$

using the sound damping coefficient Γ[3] retain the same values for Γ^* as for the commonly applied Lennard-Jones parameters (for liquids), which are listed in table 2. Thereby we obtain our ε corresponding to our σ by using the relation $\sigma^2\varepsilon = \sigma'^2\varepsilon'$ under the assumption that this law is applicable to scale from liquid to gas properties in the same way as when used between liquid properties.[4] This yields our used ε-values of $1.9654 \times 10^{-22}[J]$, $7.1957 \times 10^{-22}[J]$ and $14.9480 \times 10^{-22}[J]$ for helium, neon and argon respectively.

In Eq. (4) the first term is relatively short range and repulsive while the second is long range and attractive. In Fig. 1 the potential Φ for helium, neon and argon are plotted together with their corresponding forces, $F = -\nabla\Phi$.

In order to be able to compare the conventional definition of the mean free path given by Eq. (1) with molecular dynamics we need to declare what a collision is for the latter approach. Since molecular dynamics already uses a "closeness measure" given by

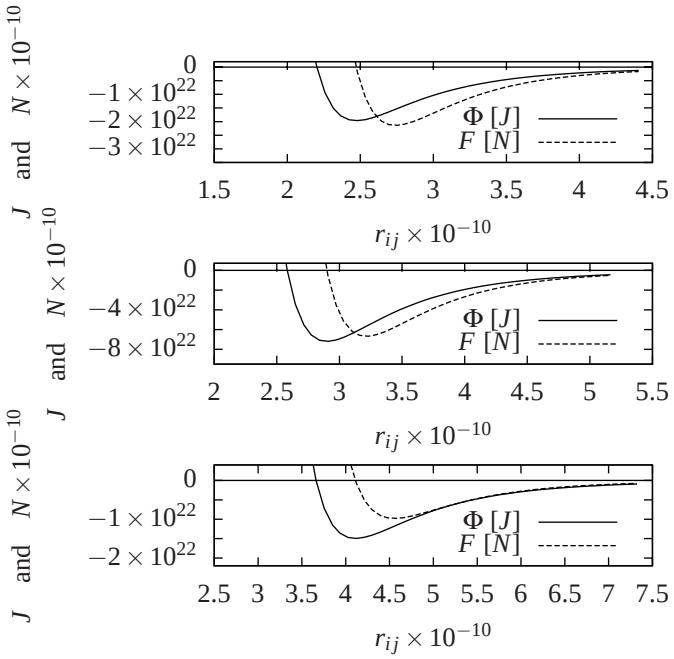

Figure 1. Potential energy $[J]$ and potential force $[N] \times 10^{-10}$ between molecules i and j of helium (top), neon (middle) and argon (bottom).

σ, we have here decided to consider a collision to have occurred if two molecules are closer to each other than this distance.

In the implementation of the recording of the mean free path we have chosen to continuously record the travelled distance of a molecule since the last collision occurred, which, when averaged over all molecules, is expected to recover the mean free path value. This modelling method is different from the intuitive method of directly measure a molecules travelled distance between two successive collisions, which only can be recorded at certain times once collisions occur. Our proposed method of recording the molecular free path for every time step carry some advantages in our investigation. One advantage is that we avoid keeping track of two successive collisions and correspondingly assigning the free path to a specific point between the positions of the two collisions. Instead the free path will be assigned to the molecules current position. Another advantage is that data recording of the free path can be made to be a molecular attribute together with pre-existing attributes such as position and velocity.

2.2 Geometry and periodic boundaries

Since we first want to validate our method we chose to obtain the unconfined value of the mean free path for helium, neon and argon gas, unaffected by any boundaries, we have chosen to simulate a cube shaped geometry with employed periodic boundaries, illustrated in Fig. 2. The periodic boundary works by trans-

[3]The sound damping coefficient is expressed as $\Gamma = [\mu/\rho + (\gamma - 1)k]/2$, where γ is the specific heat ratio and k is the heat conductivity.

[4]The sensitivity of ε on the mean free path is tested for neon gas, where it is found that when using half the value of the applied value of ε being $3.5979 \times 10^{22}[J]$ a decrease of the mean free path of about 0.16% is obtained, whereby we consider the solution being relatively insensitive to this parameter.

ferring any molecule that passes into it to a perpendicular position at the opposite boundary of the cube, retaining the same velocity.

An issue of these simulations is deciding an appropriate length of the side of the cube geometry. Ideally a large cube would be modelled but since the computational cost of molecular dynamics is severe for simulating gas at the micro scale[5] we aim to find the smallest volume of the cube that still presents reasonable results. Here we define the three simulated cube cases l_A, l_B and l_C for neon which are named after their used side-length defined by its relation to the unconfined mean free path. For neon gas this quantity is denoted, λ_{Ne}, and the corresponding simulated cube side-lengths are:

$$l_A = 0.50 \times \lambda_{\text{Ne}} \qquad l_B = 0.75 \times \lambda_{\text{Ne}} \quad \text{and} \quad l_C = 1 \times \lambda_{\text{Ne}}. \quad (8)$$

Filling the cube cases l_A, l_B and l_C requires 6084, 20520 and 51105 molecules respectively given the properties of neon at STP with a the molar mass, $M = 20.18\,[kg/kmol]$. A mesh is applied to the l_A, l_B and l_C cases consisting of 6^3, 12^3 and 16^3 cells respectively. The amount of cells are chosen so that there are more than 10 molecules on average per cell, and so that the cells are sufficiently small, as this often decrease the computational time cost [7]. Helium and argon gas are modelled using the side length of $l_B = 0.75 \times \lambda_{\text{Ne}} = 0.92475 \times 10^{-7}\,[m]$ in a mesh of $12 \times 12 \times 12$ cells containing 20520 molecules. This case corresponds to sidelengths of $0.54 \times \lambda_{\text{He}}$ and $1.5 \times \lambda_{\text{Ar}}$ for helium and argon respectively, where λ_{He} and λ_{Ar} are the unconfined mean free paths of helium and argon.

It is also interresting to investigate how many collisions by average a molecule experiences during these simulations. This is estimated by calculating the average collision time period given by:

$$\tau = \frac{\lambda}{C_{pr}}, \quad (9)$$

where

$$C_{pr} = \sqrt{2RT}, \quad (10)$$

is the most probable molecular velocity in the Gaussian velocity distribution. For the given gas conditions we get the values listed in table 3.

[5]The normal computational cost of molecular dynamics scales as the square to the amount of simulated molecules, however this molecular dynamics model has a computational cost with a linear dependency on the number of simulated molecules [6, 7].

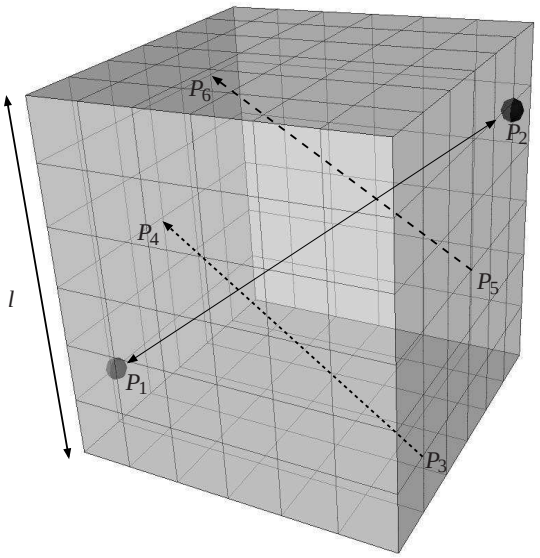

Figure 2. An example of the cube shaped simulated molecular dynamics geometry with periodic boundary conditions on all faces. The side length l is illustrated of the cube which consists of either 6^3, 12^3 or 16^3 cells for the l_A, l_B and l_C cases respectively. An example is illustrated of how a molecule travels from point P_1 to P_2 through the periodic boundaries showed by dashed arrows, in the order $P_1 \rightarrow P_3 \rightarrow P_4 \rightarrow P_5 \rightarrow P_6 \rightarrow P_2$. This travelled distance is different from the spatial difference illustrated by the solid double headed arrow between P_1 and P_2.

Table 3. Molecular data for helium, neon and argon consisting of the most probable molecular velocity, C_{pr}, the average time period between collisions, τ, and the average amount of collision per molecule during the simulated time of 3 nano seconds, N_{col}.

Gas:	He	Ne	Ar
$C_{pr}\,[m/s]$	1065.28	474.52	337.19
$\tau \times 10^{10}[s]$	2.22	2.60	1.82
N_{col}	13.5	16.5	11.6

2.3 Attributes needed for recording the free path

Due to the periodic boundary conditions it is not convenient to directly record the travelled distance of the molecule as a difference between the current position of the molecule and the position of its last collision, as illustrated in Fig. 2. Instead we obtain the molecular free path, l as follows:

$$l = (t_C - t_{LC}) \times Sp_C, \quad (11)$$

where the following attributes are used: the time of the last occurring collision, t_{LC}, the current simulated time, t_C and the current speed of the molecule, Sp_C. With these requirements we need to implement the molecular dynamics molecular attributes: t_{LC} and Col. The attribute t_{LC} is set to the current simulation time when a collision occurs. The attribute Col keeps track of whether a molecule is undergoing a collision, being activated (set to 1) if the molecule is closer to any other molecule than σ and deactivated (set to 0) if the molecules are at a distance greater than σ, in case it is already activated.

It should be noted that this recording of the mean free path does not affect the way the original molecular dynamics simulation predicts the gas behaviour.

2.4 Molecular Dynamics setup and results

The molecules are initially spatially distributed in the domain in a single cubic crystal arrangement and given a random Gaussian velocity distribution, corresponding to the set gas temperature of $273.15[K]$. The newly defined molecular dynamics attributes for recording the free path (t_C and Col) are set to zero, which is why our results of the mean free path will be zero at the start of the simulation.

We have performed two sets of measurements for the mean free path. One considers the unbounded mean free path previously described where both the mean free path when all occurring collisions are considered independent of the number of molecules taking part as well as a measurement of the mean free path where only binary collisions occur, corresponding to the theory on which the conventional definition of Eq. (1) is based. This will allow us to validate the dilute gas assumption from Eq. (2). The other set of measurements concerns the mean free path when a wall is introduced to the simulated gas, yielding specular reflections.

Experimental results considering unconfined mean free paths

In this section we model an unbounded gas package with periodic boundary conditions, where we first choose not to include any restriction of recording on the number of molecules taking part in the same collision.

In Fig. 3 we see the results of the recorded mean free paths for the l_A, l_B and l_C cases for neon and for the l_B cases for helium and argon. For the l_B cases we achieve the mean free path values for helium, neon and argon of $1.651 \times 10^{-7}[m]$, $1.221 \times 10^{-7}[m]$ and $0.625 \times 10^{-7}[m]$ respectively at the simulation time of $3 \times 10^{-9}[s]$. The achieved mean free paths by molecular dynamics differ therefor from the corresponding values of the conventional definition within about 1% for neon and argon and within about 2.5% for helium. For the l_A and l_C cases for neon we obtain a value of $1.215 \times 10^{-7}[m]$ and a value of $1.221 \times 10^{-7}[m]$ at the simulation time of $3 \times 10^{-9}[s]$ respectively. It is considered that the argon gas l_B case reassembles the best fit with the conventional values which could be explained by this gas has the shortest mean free path among the three gases, whereas the bounding box is in this respect relatively large compared to the other cases. However, all l_B gas cases has an acceptable accuracy which is why we chosen to perform all further investigation involving periodic boundaries to have a domain width of l_B (including the simulation of helium and argon).

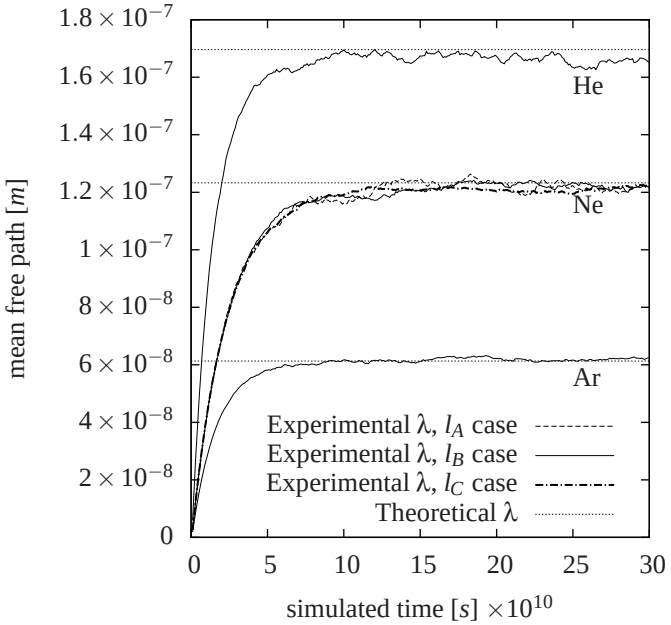

Figure 3. Convergence of the $l_A = 0.50 \times \lambda_{\mathrm{Ne}}$, $l_B = 0.75 \times \lambda_{\mathrm{Ne}}$ and $l_C = 1 \times \lambda_{\mathrm{Ne}}$ cases for neon gas and the $l_B = 0.54 \times \lambda_{\mathrm{He}}$ case for helium and the $l_B = 1.50 \times \lambda_{\mathrm{Ar}}$ case for argon, plotted against molecular dynamics simulation time. The conventional values of the mean free paths are illustrated by the straight dashed lines at values listed in table 1.

It is seen in Fig. 3 that the molecular dynamics cases with more molecules and shorter mean free paths have smoother lines of convergence to steady-state. This is because larger molecules has in general shorter free paths which causes the cell averaging to be done over a larger quantity of free paths of equal length scales. The larger cube lengths on the other hand causes a smoothening due to that the averaging is done over more molecules in the same unit of time. It should also be noted from Fig. 3 that the molecular dynamics simulation for helium, which has a longer mean free path, underpredicts the conventional value. This is probably due to that the length of the cube side is too short in relation to the free path.

We also perform an investigation where we prevent the recording of more than two molecules taking part in a collision by discarding a molecule to be considered to undergo a collision if its counter part molecule is already undergoing a collision i.e. a molecule with *Col*=0 can not collide with a molecule with $Col = 1$. In this section we have only simulated the l_B cases for helium, neon and argon where we compare the results with the theoretical mean free values of both λ by Eq. (1) and λ_k by Eq. (6). We see in Fig. 4 that all the mean free path results by molecular dynamics achieves higher values compared to when multiple molecular collisions are considered, as expected, and the results corresponds now better with the theoretical λ_k values than the theoretical λ values. The results reaches steady-state values at about a simulation time of 4.5 nano seconds as seen in Fig. 4. Due to the fluctuating values of the mean free path results an average value has been calculated for the time period between 3 nano seconds to 5 nano seconds which yielded the values of $0.652 \times 10^{-7}[m]$, $1.274 \times 10^{-7}[m]$ and $1.770 \times 10^{-7}[m]$ for helium, neon and argon respectively, which are calculated to be 6.7%, 4.2% and 4.1% higher than the results for when multiple molecular collisions are considered at 3 nano seconds. Even though these mean free path results are slightly higher then the mean free path results when multiple molecular collisions are considered we can note that the dilute gas approximation of Eq. (2) is seemingly fulfilled but might not be valid for all fields of investigations. We also see that the convergence to a steady-state occurs later, compared to when collisions by multiple molecules are taken into account. This is presumably because some collisions are discarded whereby fewer collisions are recorded per time step.

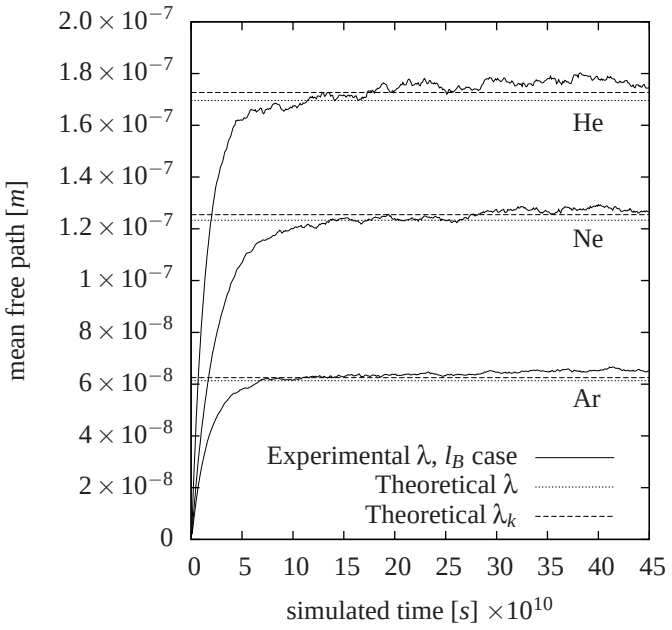

Figure 4. Convergence of the l_B cases for helium, neon and argon gases when only binary molecular collisions are taken into account, plotted against molecular dynamics simulation time. The conventional theoretical values for λ and λ_k are included for comparison.

2.5 Modelling the mean free path affected by bounding surfaces

Here we investigate the surface effects of walls on the mean free path of neon, taking into consideration that a gas molecule's collision with a wall should yield a shortening of the mean free path in the same way as if an intermolecular collision occur. We conduct such measurements in a six sided configuration using two reflective surface boundaries (in the x direction) together with two pair of periodic boundaries (in the y and z directions) see Fig. 5. The reflective surfaces are chosen to yield only specular reflections, where the molecular tangential velocity is maintained and the molecular normal velocity just changes sign.

In determining the wall effects on the free paths we will once again use the formulation for the travelled distance of a molecule since it experienced its last collision given by Eq. (11). The reflective surfaces will then be used in two different ways. Firstly and more intuitively we will use it to simulate a wall, by setting t_C to current simulated time, as done before for inter gas molecular collisions. Secondly we aim to use the reflective surfaces to simulate the bulk of the flow. This is done by setting all reflected molecules to have experienced a collisionless travel of one mean free path by setting t_C equal to the current simulated time minus $\lambda_{\mathrm{Ne}}/Sp_C$, where λ_{Ne} is the conventional mean free path for neon gas not affected by solid boundaries.

Using these reflective surfaces we examine the two cases consisting of the mean free path profile affected by a single planar wall and the mean free path profile affected by two planar walls (illustrated in figure 5).

2.5.1 Results of mean free path affected by one wall

For simulating the mean free path of the one planar wall geometry for neon gas a similar geometry to the one illustrated in Fig. 5 is used which is configured using the side lengths of $0.75 \times \lambda_{\mathrm{Ne}}$ in the y and z directions and the length $2 \times \lambda_{\mathrm{Ne}}$ in the x direction. The grading of the mesh is configured in this case so that the near wall cell widths are one forth of the width of the largest cell located at the $x = l$ position. This configuration uses 12×12 cells in the y and z direction and 40 cells in the x direction. The simulated gas is represented by 56672 molecules and the sampling of the λ_{eff} profile is made over 2 nano seconds taken after 4 nano seconds settlement, in terms of the simulated time.

The molecular dynamics results of the mean free path affected by wall collisions is compared to a theoretical model for a gas in the vicinity of one wall achieved by physical reasoning

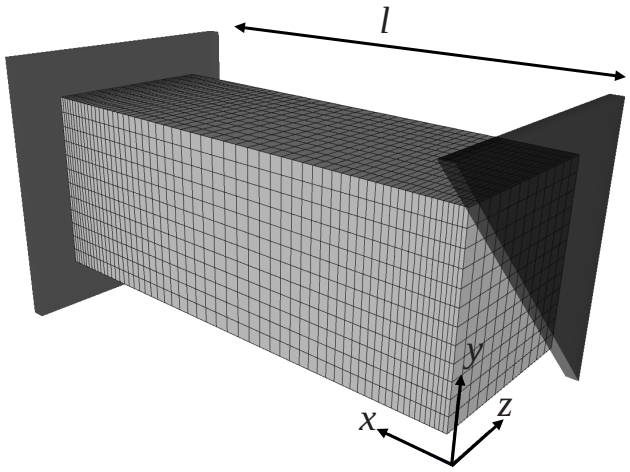

Figure 5. An example of a simulated molecular dynamics geometry with reflective surfaces in the x direction, at $x = 0$ and $x = l$. The length of the geometry extending in the x direction is denoted by l and the width and height of the geometry is $0.75 \times \lambda_{\mathrm{Ne}}$. Periodic boundary conditions are applied in the y and z directions. The mesh shown consists of $60 \times 12 \times 12$ cells in the x, y and z directions respectively. For the two planar wall case, shown here, the cells are graded in the x direction so that the cell width at $x = 0$ and at $x = l$ are one forth of the width of the cell width at $x = l/2$.

presented by E. Arlemark [3], expressed by:

$$\lambda_{\mathrm{eff}}^{T} = 1 - \frac{1}{82}\left[\exp\left(-\frac{x}{\lambda_{\mathrm{Ne}}}\right) + 4\sum_{i=1}^{7}\exp\left(-\frac{x}{\cos\left((2i-1)\pi/28\right)\lambda_{\mathrm{Ne}}}\right) + 2\sum_{i=1}^{6}\exp\left(-\frac{x}{\cos\left(\pi/14\right)\lambda_{\mathrm{Ne}}}\right)\right]. \quad (12)$$

We have also compared results with Stops [12] λ_{eff} model, considering the effects from one wall, which is described by:

$$\lambda_{\mathrm{eff}}^{St} = \frac{1}{2}\left[2 + \left(\frac{x}{\lambda} - 1\right)\exp\left(-\frac{x}{\lambda}\right) - \left(\frac{x}{\lambda}\right)^{2} Ei\left(\frac{x}{\lambda}\right)\right], \quad (13)$$

where the function Ei is the exponential integral function defined as:

$$Ei(z) = \int_{1}^{\infty} t^{-1}\exp\left(-zt\right)dt. \quad (14)$$

Also plotted in Fig. 5 is the two-term exponential curve fit to the molecular dynamics data given by:

$$\lambda_{\mathrm{eff}}^{CF} = \lambda_{\mathrm{Ne}} - \frac{\lambda_{\mathrm{Ne}}}{2}\left[0.4561\exp\left(\frac{-5.850x}{\lambda_{\mathrm{Ne}}}\right) + 0.5706\exp\left(\frac{-1.039x}{\lambda_{\mathrm{Ne}}}\right)\right]. \quad (15)$$

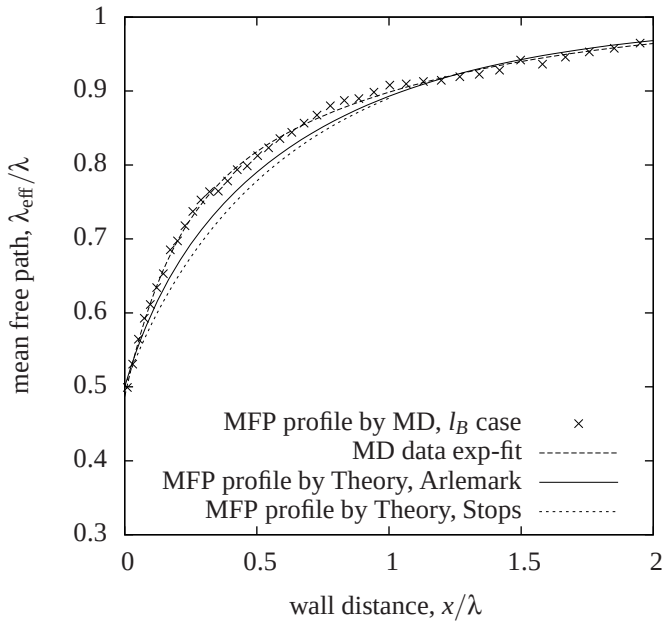

Figure 6. Mean free path profile achieved by Molecular Dynamics and achieved by theoretical model from physical reasoning.

It can be seen in Fig. 5 That the theoretical models achieves the same near wall values and bulk values as the values achieved by the molecular dynamics simulation. However the results of the λ_{eff} profile from the molecular dynamics simulation is slightly higher than the theoretical models at approximately the wall distance of $x = 0.5/\lambda_{\mathrm{Ne}}$.

2.5.2 Results of mean free path effected by two walls

In this section the reflective surface at $x = l$ is repaced with a planar wall yielding specular reflections. The simulated geometry has a side length of $0.75 \times \lambda_{\mathrm{Ne}}$ in the y and z directions and $2 \times \lambda_{\mathrm{Ne}}$ and $1 \times \lambda_{\mathrm{Ne}}$ in the x direction representing simulations of $Kn = 0.5$ and $Kn = 1$ cases.

The λ_{eff} profile from the molecular dynamics simulation is presented together with the theoretical model for a gas in a two

wall confinement achieved by physical reasoning presented by E. Arlemark [3], expressed by:

$$\begin{aligned}\lambda_{\text{eff}}^{T} =&\lambda_{\text{Ne}} - \frac{\lambda_{\text{Ne}}}{82}\left[\exp\left(-\frac{x}{\lambda_{\text{Ne}}}\right) + \exp\left(-\frac{l-x}{\lambda_{\text{Ne}}}\right)\right.\\ &+4\sum_{i=1}^{7}\exp\left(-\frac{x}{\lambda_{\text{Ne}}\cos\left[(2i-1)\pi/28\right]}\right)\\ &+4\sum_{i=1}^{7}\exp\left(-\frac{l-x}{\lambda_{\text{Ne}}\cos\left[(2i-1)\pi/28\right]}\right)\\ &+2\sum_{i=1}^{6}\exp\left(-\frac{x}{\lambda_{\text{Ne}}\cos\left[\pi i/14\right]}\right)\\ &\left.+2\sum_{i=1}^{6}\exp\left(-\frac{l-x}{\lambda_{\text{Ne}}\cos\left[\pi i/14\right]}\right)\right]. \end{aligned} \tag{16}$$

We have included Stops [12] λ_{eff} model for two walls for comparison which is described by:

$$\begin{aligned}\lambda_{\text{eff}}^{St} =&\frac{1}{2}\left[2+\left(\frac{x}{\lambda}-1\right)\exp\left(-\frac{x}{\lambda}\right)-\left(\frac{x}{\lambda}\right)^2 Ei\left(\frac{x}{\lambda}\right)\right.\\ &\left.+\left(\frac{l-x}{\lambda}-1\right)\exp\left(\frac{l-x}{\lambda}\right)-\left(\frac{l-x}{\lambda}\right)^2 Ei\left(\frac{l-x}{\lambda}\right)\right]. \end{aligned} \tag{17}$$

We also use the molecular dynamics curve fit data of the λ_{eff} profile for one wall presented by Eq. (15), which we reformulate in an attempt to predict the λ_{eff} profile for two walls as follows:

$$\begin{aligned}\lambda_{\text{eff}}^{CF} =&\lambda_{\text{Ne}} - \frac{\lambda_{\text{Ne}}}{2}\left[0.4561\exp\left(\frac{-5.850x}{\lambda_{\text{Ne}}}\right)\right.\\ &+0.5706\exp\left(\frac{-1.039x}{\lambda_{\text{Ne}}}\right)\\ &+0.4561\exp\left(\frac{-5.850(l-x)}{\lambda_{\text{Ne}}}\right)\\ &\left.+0.5706\exp\left(\frac{-1.039(l-x)}{\lambda_{\text{Ne}}}\right)\right], \end{aligned} \tag{18}$$

using similar reasoning as for the theoretical model of Eq. (16).

The results of the molecular dynamics λ_{eff} profile is plotted in Fig. 7 together with the modified curve fit data for two walls represented by Eq. (18). In addition the theoretical models for the λ_{eff} profiles given by Eq. (16) and Eq. (17) are plotted in Fig. 7. All the λ_{eff} profiles described above are presented in Fig. 7 for $Kn = 0.5$ and $Kn = 1$. Whereas an additional comparison is made using just the two wall curve fit model of Eq. (18) and the two wall theoretical models of Eq. (16) and Eq. (17) for $Kn = 0.2$. It is seen that the three λ_{eff} profiles all have about the same near wall value while the bulk values differs significantly, except for the $Kn = 0.2$ case. In the $Kn = 0.5$ case the curve fit data matches the data from the molecular dynamics simulation the best in the near wall area but the theoretical model the best in the bulk. The separation between the λ_{eff} profile from the molecular dynamics simulation is the most different from the theoretical models for the $Kn = 1$ case, where the curve fit model represents the values of the molecular dynamics data the best throughout the simulated domain.

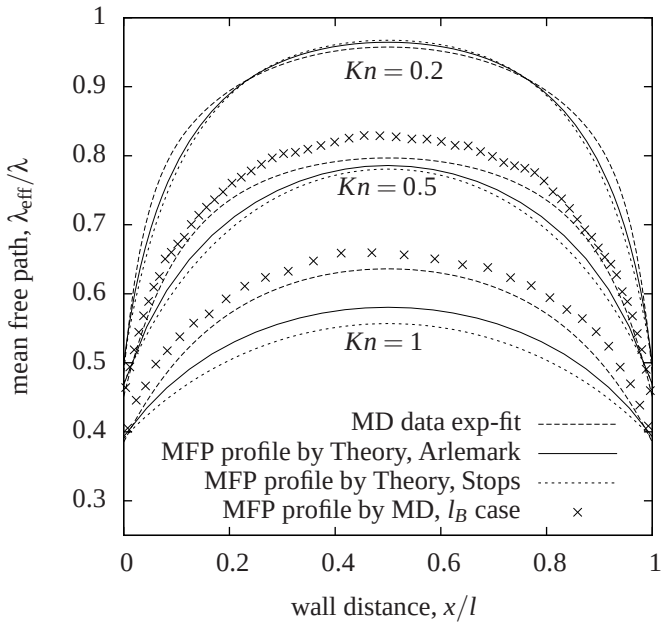

Figure 7. Mean free path profile achieved by molecular dynamics, theoretical model achieved by from physical reasoning and mean free path curve fit model from one wall molecular dynamics simulation.

3 DISCUSSION AND CONCLUSIONS

In this paper we use molecular dynamics to record the molecular travelling distances between collisions of helium, neon and argon gases at standard temperature and pressure conditions and compare with corresponding conventional theoretical values. If we record the molecular free paths that are due to multiple molecular collisions we achieve steady-state values for the unconfined mean free paths which are within 1% accuracy for argon and neon and within 2.5% accuracy for helium compared to the conventional theoretical values. However, if we record the

mean free paths for molecules that only experiences binary collisions we find that these steady-state results are 6.7%, 4.2% and 4.1% higher than the results where all collisions are considered. This difference might be significant in some cases yielding that the dilute gas approximation might not always be valid. Planer walls with specular reflection characteristics are introduced to the simulated molecular dynamics geometry and the mean free path is recorded at various wall distances in order to compare with physically derived models. It is found that the theoretical models and the molecular dynamics method show similar results for singular wall geometries and two parallel planar wall cases up to Knudsen numbers of about 0.2.

We conclude that we are capable of reproducing the unconfined mean free path values of the conventional expression using molecular dynamics and in addition model how the mean free path varies with distance to a wall which is compared to various theoretical models. Such results will prove useful as the modelling of micro-gas-flows using Navier-Stokes equations can be done by incorporating a non-linear stress/strain rate relationship with knowledge of the variation of the mean free path with wall distance [3]. The knowledge of the affect of walls on the mean free path will also be useful for the boundary conditions of Navier-Stokes equations because they are dependent on a near wall value of the mean free path.

Altough we have managed to capture some of the theoretical predictions of the mean free path using molecular dynamics further investigation on various types of gas molecular collisions with walls could yield better understanding of, for instance, second order effects concerning not only specular collisions but also diffusive reflections and mixtures of these reflections.

ACKNOWLEDGMENT

The authors would like to thank Graham Macpherson and Matthew Borg for helpful discussions. This research is funded in the UK by the Engineering and Physical Sciences Research Council under grant number EP/D007488/1.

REFERENCES

[1] Cercignani, C., 2000. *Rarefied Gas Dynamics: from Basic Concepts to Actual Calculations*. Cambridge University Press.

[2] Kandlikar, S., Garimella, S., Li, D., Colin, S., and King, M. R., 2005. *Heat Transfer and Fluid Flow in Minichannels and Microchannels*. Elsevier.

[3] Arlemark, E. J., Dadzie, S. K., and Reese, J. M. "an extension to the Navier-Stokes equations to incorporate gas molecular collisions with boundaries". to be published in Journal of Heat Transfer.

[4] Nordling, C., and Österman, J., 1999. *Physics Handbook: for Science and Engineering*, 6 ed. Studentlitteratur.

[5] OpenFOAM, the Open Source CFD Toolbox, http://www.opencfd.co.uk.

[6] Macpherson, G. B., and Reese, J. M., 2008. "Molecular dynamics in arbitrary geometries: parallel evaluation of pair forces". *Molecular Simulation*, **34**(1), pp. 97–115.

[7] Macpherson, G. B., Borg, M. K., and Reese, J. M., 2007. "Parallel generation of molecular dynamics initial configurations in arbitrary geometries". *Molecular Simulation*, **33**(15), pp. 1199–1212.

[8] Karniadakis, G., Beskok, A., and Aluru, N., 2005. *Microflows and Nanoflows: Fundamentals and Simulation*. Springer.

[9] Bird, R. B., Stewart, W. E., and Lightfoot, E. N., 2003. *Molecular Gas Dynamics and the Direct Simulation of Gas Flows*. Oxford Science Publications.

[10] Bird, G. A., 2003. *Molecular Gas Dynamics and the Direct Simulation of Gas Flows*. Oxford Science Publications.

[11] Guarini, E., Bafile, U., Barocchi, F., Demmel, F., Formisano, F., Sampoli, M., and Venturi, G., 2005. "Collective excitations in liquid cd4: Neutron scattering and molecular-dynamics simulations". *Europhysics Letters*, **72**(6), pp. 969–975.

[12] Stops, D. W., 1970. "The mean free path of gas molecules in the transition regime". *Journal of Physics D*, **3**(5), pp. 685–696.